IOPscience iopscience.iop.org

Home Search Collections Journals About Contact us My IOPscience

Solution of the linearised Vlasov equation for collisionless plasmas evolving in external fields of arbitrary spatial and time dependence. II

This article has been downloaded from IOPscience. Please scroll down to see the full text article.

1990 J. Phys. A: Math. Gen. 23 2463

(http://iopscience.iop.org/0305-4470/23/12/025)

View the table of contents for this issue, or go to the journal homepage for more

Download details:
IP Address: 129.252.86.83
The article was downloaded on 31/05/2010 at 14:25

Please note that terms and conditions apply.

J. Phys. A: Math. Gen. **23** (1990) 2463-2478. Printed in the UK

Solution of the linearised Vlasov equation for collisionless plasmas evolving in external fields of arbitrary spatial and time dependence II

V Škarka†§ and P V Coveney‡

† International Centre for Theoretical Physics, Trieste, Italy
‡ Department of Chemistry, University of Wales, Bangor LL57 2UW, UK

Received 22 December 1989

Abstract. We solve perturbatively the linearised Vlasov equation describing inhomogeneous collisionless plasmas evolving in time-dependent external fields. The method employs an explicitly time-dependent formalism and is facilitated by the use of diagrammatic techniques. It leads to a straightforward algorithm for computing the contribution to the solution, order by order in the external field. In the previous paper we provided the solution to first order; higher orders are described in the present paper.

1. Introduction

This paper is a continuation of the immediately preceding one (Škarka and Coveney 1990), henceforth referred to as I, and should be read in conjunction with it. In that paper, we used a perturbational method to solve the linearised Vlasov equation describing collisionless plasmas evolving in quite general external fields of arbitrary spatial and time dependence. The analysis given there, which is heavily based on statistical mechanical diagram techniques (Balescu 1963), was carried out explicitly to first order with respect to the external field (but to all orders with respect to the internal interactions). In the present paper, we extend the treatment to higher orders.

In first order (with respect to the external field), one has only to deal with single-line diagrams, yet a glance at figure 2 of I shows that in higher orders there are contributions from diagrams comprising more than one line. Such diagrams present some qualitatively new features which are described in this paper. However, the essential point which emerges, despite the greater complexity now present, is that there is still a regular structure to the contributions, order by order in the external field.

In section 2, we obtain a general expression for the contribution from single-line diagrams with two external-field (EF) vertices which follows along exactly the same lines as described in I. Section 3 deals with the new situation that pertains when, at second order, there are two lines present. Higher-order contributions are calculated in section 4, and we end the paper with some general conclusions in section 5.

2. Extension of the general formula to diagrams with two external-field vertices on a line

We remarked in I (section 4) that the general formulae (4.25) and (4.26) are actually of considerably greater generality than might be apparent from the restricted context

§ Permanent address: Institute of Physics, PO Box 57, 11001 Beograd, Yugoslavia.

0305-4470/90/122463+16$03.50 © 1990 IOP Publishing Ltd

of first-order diagrams alone. In fact, at orders higher than first, we do not need to begin a new computation of the corresponding expressions *ab initio*. Indeed, we noted that the structure of the diagrams (figure 2 of I) suggests that in higher order there will be a repetition of the single EF vertex patterns which we studied in I.

Recall that EF vertices connect the parts of a diagram contributing to different first level subdynamics. For instance, the diagram with two EF vertices (in figure 1) contributes to three different subdynamics. Already on this subdynamics level we sum the internal field (IF) interactions to all orders in the coupling constant $\lambda = e^2$ (equations (2.2) and (4) of I). Thus, in computing generalised subdynamics, which deals with the action of the external field, only propagators directly associated with first level subdynamics, i.e. coming from the part of the diagram labelled by S_i in figure 1 (with $i = 0, 1, 2, \ldots$), are involved. Taking this into account, our aim is now to show how the general formula for two EF vertex sequences on a line arises from that for one EF vertex alone.

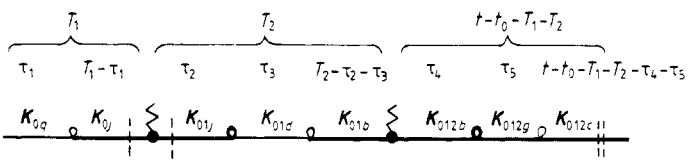

Figure 1. A particular diagram in the class {0} (shown in figure 2 of I).

In order to realise this objective, we first consider one particular diagram from the whole class {0} (in figure 2 of I), as shown in figure 1. This diagram is related one-to-one to the corresponding part of the solution of the Vlasov equation:

$$
\begin{aligned}
h_{\boldsymbol{K}_{0a}}(t) \doteq \int \mathrm{d}\Gamma \int_0^{t-t_0} \mathrm{d}T_1 \, \mathrm{e}^{[\mathrm{i}(\omega_{12}-\boldsymbol{K}_0\cdot\boldsymbol{v}_j+\boldsymbol{K}_{012}\cdot\boldsymbol{v}_c)T_1]} \\
\times \int_0^{t-t_0-T_1} \mathrm{d}T_2 \, \mathrm{e}^{[\mathrm{i}(\omega_2-\boldsymbol{K}_{01}\cdot\boldsymbol{v}_b+\boldsymbol{K}_{012}\cdot\boldsymbol{v}_c)T_2]} \\
\times \int_0^{+\infty} \mathrm{d}\tau_1 \, \mathrm{e}^{[-(\xi+\mathrm{i}\boldsymbol{K}_0\cdot\boldsymbol{v}_{aj})\tau_1]} \mathscr{V}_{0a} \boldsymbol{F}_{1j} \cdot \frac{\partial}{\partial \boldsymbol{v}_j} \\
\times \int_0^{-\infty} \mathrm{d}\tau_3 \, \mathrm{e}^{[(\xi-\mathrm{i}\boldsymbol{K}_{01}\cdot\boldsymbol{v}_{db})\tau_3]} \mathscr{V}_{1d} \\
\times \int_{+\infty}^{T_2-\tau_3} \mathrm{d}\tau_2 \, \mathrm{e}^{[-(\xi+\mathrm{i}\boldsymbol{K}_{01}\cdot\boldsymbol{v}_{jb})\tau_2]} \mathscr{V}_{1j} \boldsymbol{F}_{2b} \cdot \frac{\partial}{\partial \boldsymbol{v}_b} \\
\times \int_0^{+\infty} \mathrm{d}\tau_4 \, \mathrm{e}^{[-(\xi+\mathrm{i}\boldsymbol{K}_{012}\cdot\boldsymbol{v}_{bc})\tau_4]} \mathscr{V}_{2b} \\
\times \int_0^{+\infty} \mathrm{d}\tau_5 \, \mathrm{e}^{[-(\xi+\mathrm{i}\boldsymbol{K}_{012}\cdot\boldsymbol{v}_{gc})\tau_5]} \mathscr{V}_{2g} \\
\times \mathrm{e}^{[-\mathrm{i}\boldsymbol{K}_{012}\cdot\boldsymbol{v}_c(t-t_0)]} f_{\boldsymbol{K}_{012}}(\boldsymbol{v}_c;\, t_0). \qquad (2.1)
\end{aligned}
$$

For reasons of space, we do not provide all the details here, but instead we give directly the expression for the generalised subdynamics which was obtained according to the

choice of the first level subdynamics made in figure 1 (indicated by dotted vertical lines), using the usual procedure of computation (see I):

$$h_{\boldsymbol{K}_{0a}}(t) \doteq \int \mathrm{d}\Gamma \frac{1}{\mathrm{i}\xi - \boldsymbol{K}_0 \cdot \boldsymbol{v}_{aj}} \mathscr{V}_{0a} \frac{(-1)}{\mathrm{i}\xi + \omega_{12} - \boldsymbol{K}_0 \cdot \boldsymbol{v}_j + \boldsymbol{K}_{012} \cdot \boldsymbol{v}_c} \boldsymbol{F}_{1j} \cdot \frac{\partial}{\partial \boldsymbol{v}_j}$$
$$\times \frac{1}{\mathrm{i}\xi + \omega_2 - \boldsymbol{K}_{01} \cdot \boldsymbol{v}_j + \boldsymbol{K}_{012} \cdot \boldsymbol{v}_c} \mathscr{V}_{1j} \frac{1}{-\mathrm{i}\xi - \boldsymbol{K}_{01} \cdot \boldsymbol{v}_{dj}} \mathscr{V}_{1d} \frac{1}{-\mathrm{i}\xi - \boldsymbol{K}_{01} \cdot \boldsymbol{v}_{bj}} \boldsymbol{F}_{2b} \cdot \frac{\partial}{\partial \boldsymbol{v}_b}$$
$$\times \frac{1}{\mathrm{i}\xi - \boldsymbol{K}_{012} \cdot \boldsymbol{v}_{bc}} \mathscr{V}_{b2} \frac{1}{\mathrm{i}\xi - \boldsymbol{K}_{012} \cdot \boldsymbol{v}_{gc}} \mathscr{V}_{g2}$$
$$\times \mathrm{e}^{[-\mathrm{i}\boldsymbol{K}_{012} \cdot \boldsymbol{v}_c (t - t_0)]} f_{\boldsymbol{K}_{012}}(\boldsymbol{v}_c; t_0). \tag{2.2}$$

The first subdynamical propagator (belonging to the term S_0) is of the same form as those in section 4 of I except that it contains the sum of ω_1 and ω_2, since it is separated from the second level subdynamical propagator (E) by two external field terms, F_1 and F_2, respectively. The second subdynamical propagator (S_2) is separated from E by F_2 only; consequently it carries the corresponding frequency ω_2. This is all that has to be added in order to be able to write down the general formula for the contribution of the whole class {0} of two EF vertex diagrams (i.e. the diagrams with all possible numbers of loops) represented in figure 2. To write down this contribution, we use the first-order result of (4.25) derived in I together with the second-order expression (2.2) in which, between each subdynamics propagator S_i and EF vertex term, an arbitrary number of internal field terms is added:

$$h_{\boldsymbol{K}_{x\alpha}}(t) \doteq \int \mathrm{d}\Gamma \frac{1}{\varepsilon(\boldsymbol{K}_x)} \frac{1}{\mathrm{i}\xi - \boldsymbol{K}_x \cdot \boldsymbol{v}_\sigma + \boldsymbol{K}_{xyz} \cdot \boldsymbol{v}_\Sigma + \omega_{yz}} \mathscr{V}_{x\sigma} \frac{1}{\varepsilon^{\mathrm{cc}}(\boldsymbol{K}_x)}$$
$$\times \frac{1}{-\mathrm{i}\xi - \boldsymbol{K}_x \cdot \boldsymbol{v}_{\beta\sigma}} \boldsymbol{F}_{y\beta} \cdot \frac{\partial}{\partial \boldsymbol{v}_\beta} \frac{1}{\mathrm{i}\xi - \boldsymbol{K}_{xy} \cdot \boldsymbol{v}_{\beta\eta}} \mathscr{V}_{y\beta} \frac{1}{\varepsilon(\boldsymbol{K}_{xy})}$$
$$\times \frac{1}{\mathrm{i}\xi - \boldsymbol{K}_{xy} \cdot \boldsymbol{v}_\eta + \boldsymbol{K}_{xyz} \cdot \boldsymbol{v}_\Sigma + \omega_z} \mathscr{V}_{y\eta} \frac{1}{\varepsilon^{\mathrm{cc}}(\boldsymbol{K}_{xy})} \frac{1}{-\mathrm{i}\xi - \boldsymbol{K}_{xy} \cdot \boldsymbol{v}_{y\eta}}$$
$$\times \boldsymbol{F}_{z\gamma} \cdot \frac{\partial}{\partial \boldsymbol{v}_\gamma} \frac{1}{\mathrm{i}\xi - \boldsymbol{K}_{xyz} \cdot \boldsymbol{v}_{\gamma\Sigma}} \mathscr{V}_{z\gamma} \frac{1}{\varepsilon(\boldsymbol{K}_{xyz})} \mathrm{e}^{[-\mathrm{i}\boldsymbol{K}_{xyz} \cdot \boldsymbol{v}_\Sigma (t - t_0)]}$$
$$\times \mathscr{V}_{z\Sigma} \frac{1}{\varepsilon^{\mathrm{cc}}(\boldsymbol{K}_{xyz})} \frac{1}{-\mathrm{i}\xi - \boldsymbol{K}_{xyz} \cdot \boldsymbol{v}_{\nu\Sigma}} f_{\boldsymbol{K}_{xyz}}(\boldsymbol{v}_\nu; t_0). \tag{2.3}$$

Let us now illustrate the utilisation of this general formula in order to obtain an explicit contribution directly from a given diagram with a particular choice of subdynamics. The choice of subdynamics in figure 2 is of 'type I' (following the terminology introduced in I), i.e. the generalised sybdynamics is associated with the propagator ($S_2 = E$) which does not share a particle with the external field derivative ($E \not\subset F_1$). For this choice of subdynamics, we can write down directly the corresponding explicit algebraic expression using the algorithm stated in section 4 of I so as to complete the

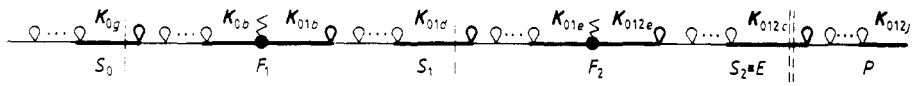

Figure 2. Diagrams with all possible numbers of loops in the class {0}.

general formula (2.3) with appropriate indices from the diagram in figure 2. The algorithm is based on the correspondence between the final expression obtained when all convolution integrals are done and the corresponding diagram, which is itself related one-to-one with the original algebraic expression (as written in (2.1)).

As will be recalled from I, in implementing the algorithm we proceed from left to right. In the plasma dielectric function appearing furthest to the left in (2.3), we replace the wavevector by the one read from the propagator occurring at the extreme left in the diagram. Next comes the propagator associated with the subdynamics lying furthest to the left. The wavevector and particle index of its first eigenvalue $\boldsymbol{K}_x \cdot \boldsymbol{v}_\sigma$ are replaced by those of this subdynamics propagator (indicated in the diagram by a dotted vertical line). The second eigenvalue always carries the indices of the propagator associated with the generalised subdynamics E (indicated by two dotted lines). The indices of the frequencies ω_1 and ω_2 in the sum ω_{12} correspond respectively to the wavevector indices of EF vertices F_1 and F_2. This propagator is followed by the internal field (IF) term which depends on the same wavevector and particle as the corresponding vertex in the diagram. Repeating the same prescription, the whole contribution of the diagram can be written explicitly

$$
\begin{aligned}
h_{\boldsymbol{K}_{0a}}(t) \doteq \int \mathrm{d}\Gamma\, & \frac{1}{\varepsilon(\boldsymbol{K}_0)} \frac{1}{\mathrm{i}\xi - \boldsymbol{K}_0 \cdot \boldsymbol{v}_g + \boldsymbol{K}_{012} \cdot \boldsymbol{v}_c + \omega_{12}} \mathscr{V}_{0g} \frac{1}{\varepsilon^{\mathrm{cc}}(\boldsymbol{K}_0)} \frac{1}{-\mathrm{i}\xi - \boldsymbol{K}_0 \cdot \boldsymbol{v}_{bg}} \\
& \times \boldsymbol{F}_{1b} \cdot \frac{\partial}{\partial \boldsymbol{v}_b} \frac{1}{\mathrm{i}\xi - \boldsymbol{K}_{01} \cdot \boldsymbol{v}_{bd}} \mathscr{V}_{1b} \frac{1}{\varepsilon(\boldsymbol{K}_{01})} \frac{1}{\mathrm{i}\xi - \boldsymbol{K}_{01} \cdot \boldsymbol{v}_d + \boldsymbol{K}_{012} \cdot \boldsymbol{v}_c + \omega_2} \\
& \times \mathscr{V}_{1d} \frac{1}{\varepsilon^{\mathrm{cc}}(\boldsymbol{K}_{01})} \frac{1}{-\mathrm{i}\xi - \boldsymbol{K}_{01} \cdot \boldsymbol{v}_{ed}} \boldsymbol{F}_{2e} \cdot \frac{\partial}{\partial \boldsymbol{v}_e} \frac{1}{\mathrm{i}\xi - \boldsymbol{K}_{012} \cdot \boldsymbol{v}_{ec}} \mathscr{V}_{2e} \frac{1}{\varepsilon(\boldsymbol{K}_{012})} \\
& \times \mathrm{e}^{[-\mathrm{i}\boldsymbol{K}_{012} \cdot \boldsymbol{v}_c (t - t_0)]} \mathscr{V}_{2c} \frac{1}{\varepsilon^{\mathrm{cc}}(\boldsymbol{K}_{012})} \frac{1}{-\mathrm{i}\xi - \boldsymbol{K}_{012} \cdot \boldsymbol{v}_{pc}} f_{\boldsymbol{K}_{012}}(\boldsymbol{v}_p;\, t_0). \qquad (2.4)
\end{aligned}
$$

In paper I there were two distinct cases concerning the choice of the first level subdynamics for type-I generalised subdynamics. Namely, the propagator associated with the subdynamics furthest to the left either shares a particle with the EF vertex or it does not. The addition of an extra EF vertex creates four possible ways of choosing the intermediate first level subdynamics (including the situation where there are no loops between external field vertices because the parts of the diagram F_1 and F_2 overlap—denoted $F_{S_1 S_1} F$). There are therefore eight particular cases. To these we add the eight cases coming from the type-II choice of generalised subdynamics where the propagator ($S_3 = E$) associated with the generalised subdynamics is immediately adjacent to the EF vertex lying furthest to the right, denoted F_E in I.

Taking into account all these particular choices of subdynamics, the sum over all subdynamics to which the diagram in figure 2 contributes can be represented symbolically as

$$
\begin{aligned}
\frac{1}{\varepsilon}\Bigg\{ & \left({}_{S_0}F + S_0 \frac{1}{\varepsilon^{\mathrm{cc}}} F \right) \frac{1}{\varepsilon} \left[\left({}_{S_1}F + S_1 \frac{1}{\varepsilon^{\mathrm{cc}}} F \right) \frac{1}{\varepsilon} E + {}_{S_1}F_E + S_0 \frac{1}{\varepsilon^{\mathrm{cc}}} F_E \right] + \left({}_{S_0}F_{S_1} + S_0 \frac{1}{\varepsilon^{\mathrm{cc}}} F_{S_1} \right) \\
& \left[\frac{1}{\varepsilon^{\mathrm{cc}}} \left(F_E + F \frac{1}{\varepsilon} E \right) + {}_{S_1}F_E + {}_{S_1}F \frac{1}{\varepsilon} E \right] \Bigg\} \frac{1}{\varepsilon^{\mathrm{cc}}} P. \qquad (2.5)
\end{aligned}
$$

In order to write an explicit expression from this symbolic formula, we recall the convention established in I that each time the propagator S_0 precedes an EF vertex region labelled F_E in the symbolic formula, their order must be permuted in the explicit expression. But now we have one more EF vertex between the propagator S_0 and F_E. However, in the particular situation denoted ${}_{S_0}F$, the propagator S_0 precedes the derivative associated with this EF vertex, whilst sharing the same particle with it. In this case the velocity derivative does not operate on this propagator and we must ensure that it does not so act when, in the explicit expression, the propagator S_0 is placed to the right of the next EF derivative. We can do this by introducing brackets with superscripts (see (2.6) below). For the same reason, the subdynamics propagator S_1 also has to be placed on the right of the EF derivative in the explicit expression.

In the particular case when S_0 belongs to the region F_E (denoted ${}_{S_0}F_E$), an extra term in square brackets has to be added in front of this propagator, owing to the non-commutation between the propagator S_0 and the velocity derivative in F_E (which arises because they share the same particle), in accordance with the algorithm explained in I. Furthermore, if a subdynamics propagator S_i belongs to an EF vertex region F_i there are no loop vertices between the two: in such a case, the corresponding inverse plasma dielectric function $(1/\varepsilon)$ in (2.3) must be omitted.

Therefore, taking into account the symbolic formula (equation (2.5)) together with the general algebraic expression (equation (2.3)) we now obtain the complete, explicit contribution to the solution of the linearised Vlasov equation from all single-line diagrams at second order with respect to the external field:

$$
\begin{aligned}
h_{\boldsymbol{K}_{x\alpha}}(t) \doteq \int \mathrm{d}\Gamma\, & \frac{1}{\varepsilon(\boldsymbol{K}_x)} \left\{ \delta_{\beta\sigma} + (1-\delta_{\beta\sigma}) \mathscr{V}_{x\sigma} \frac{1}{\varepsilon^{\mathrm{cc}}(\boldsymbol{K}_x)} \frac{1}{-\mathrm{i}\xi - \boldsymbol{K}_x \cdot \boldsymbol{v}_{\beta\sigma}} \right\} \boldsymbol{F}_{y\beta} \cdot \frac{\partial^{(1)}}{\partial \boldsymbol{v}_\beta} \\
& \times \left\{ \delta_{\beta\eta} + (1-\delta_{\beta\eta}) \frac{1}{\mathrm{i}\xi - \boldsymbol{K}_{xy} \cdot \boldsymbol{v}_{\beta\eta}} \mathscr{V}_{y\beta} \frac{1}{\varepsilon(\boldsymbol{K}_{xy})} \right\} \\
& \times \left\{ \delta_{\gamma\eta} + (1-\delta_{\gamma\eta}) \mathscr{V}_{y\eta} \frac{1}{\varepsilon^{\mathrm{cc}}(\boldsymbol{K}_{xy})} \frac{1}{\mathrm{i}\xi - \boldsymbol{K}_{xy} \cdot \boldsymbol{v}_{\gamma\eta}} \right\} \\
& \times \boldsymbol{F}_{z\gamma} \cdot \left\{ \delta_{\gamma\Sigma} \frac{\partial^{(3)}}{\partial \boldsymbol{v}_\gamma} [0]^{(\delta_{\sigma\beta})} \left[\frac{\boldsymbol{K}_{xyz}}{\boldsymbol{K}_{yz}} \right]^{(\delta_{\sigma\Sigma})} \left[\frac{\boldsymbol{K}_{xyz}}{\boldsymbol{K}_{yz}} \right]^{(2+\delta_{\sigma\Sigma})} \right. \\
& \times \frac{1}{\mathrm{i}\xi - \boldsymbol{K}_x \cdot \boldsymbol{v}_\sigma + \boldsymbol{K}_{xyz} \cdot \boldsymbol{v}_\Sigma + \omega_{yz}} \left[\frac{\boldsymbol{K}_{xyz}}{\boldsymbol{K}_z} \right]^{(2+\delta_{\eta\Sigma})} \frac{1}{\mathrm{i}\xi - \boldsymbol{K}_{xy} \cdot \boldsymbol{v}_\eta + \boldsymbol{K}_{xyz} \cdot \boldsymbol{v}_\Sigma + \omega_z} \\
& + (1-\delta_{\gamma\Sigma})[0]^{(\delta_{\sigma\beta})} \frac{1}{\mathrm{i}\xi - \boldsymbol{K}_x \cdot \boldsymbol{v}_\sigma + \boldsymbol{K}_{xyz} \cdot \boldsymbol{v}_\Sigma + \omega_{yz}} \\
& \left. \times \frac{1}{\mathrm{i}\xi - \boldsymbol{K}_{xy} \cdot \boldsymbol{v}_\eta + \boldsymbol{K}_{xyz} \cdot \boldsymbol{v}_\Sigma + \omega_z} \frac{\partial}{\partial \boldsymbol{v}_\gamma} \frac{1}{\mathrm{i}\xi - \boldsymbol{K}_{xyz} \cdot \boldsymbol{v}_{\gamma\Sigma}} \mathscr{V}_{z\gamma} \frac{1}{\varepsilon(\boldsymbol{K}_{xyz})} \right\} \\
& \times \mathrm{e}^{[-\mathrm{i}\boldsymbol{K}_{xyz} \cdot \boldsymbol{v}_\Sigma (t-t_0)]} \mathscr{V}_{z\Sigma} \frac{1}{\varepsilon^{\mathrm{cc}}(\boldsymbol{K}_{xyz})} \\
& \times \frac{1}{-\mathrm{i}\xi - \boldsymbol{K}_{xyz} \cdot \boldsymbol{v}_{\nu\Sigma}} f_{\boldsymbol{K}_{xyz}}(\boldsymbol{v}_\nu; t_0)
\end{aligned}
\tag{2.6}
$$

where, with reference to what was said above and for the sake of compactness, we have introduced square brackets with superscripts (1) and (3) (Škarka 1989a, b). By definition, when a derivative carrying such a superscript acts on the propagator preceded

by a square bracket with the same superscript, this propagator has to be multiplied by the expression inside the bracket (see equation (4.17) of I). When this derivative acts on other propagators no multiplication occurs if either there are no square brackets preceding them or the brackets carry different superscripts.

Thus, expressions (4.21) of I and (2.6) of the present paper taken together provide the complete contribution from all one-line diagrams to the solution of the linearised Vlasov equation, up to second order in the external field.

3. Second-order diagrams with two lines

In the diagrammatic representation, the lowest order with respect to the external field for which two lines can appear is the second one. This is a consequence of the fact that, for the linearised Vlasov equation, the second (and any additional) lines must start and end with an EF vertex (see I). Therefore, in this case, the upper line contains only loop vertices ($\{V\}$ in figure 2 of I). For example, consider two particular diagrams from the class $\{V\}$, as shown in figure 3.

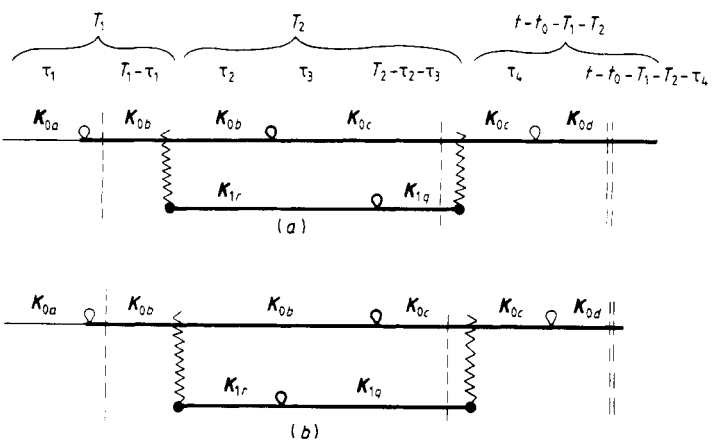

Figure 3. A particular pair of diagrams corresponding to the simplest permutation class of diagrams in the class $\{Q\}$.

Diagrams such as these with two EF vertices are divided by them into three parts, each of which contributes to a separate subdynamics. Thus, the contribution of the diagram (a) in figure 3

$$h_{K_{0a}}(t) \doteq \int \mathrm{d}\boldsymbol{v}_a \int \mathrm{d}\boldsymbol{v}_b \int \mathrm{d}\boldsymbol{v}_c \int \mathrm{d}\boldsymbol{v}_d \int \mathrm{d}\boldsymbol{v}_r \int \mathrm{d}\boldsymbol{v}_q \int_0^{t-t_0} \mathrm{d}T_1 \int_0^{T_1} \mathrm{d}\tau_1 \, \mathrm{e}^{(-\mathrm{i}\boldsymbol{K}_0 \cdot \boldsymbol{v}_a \tau_1)}$$

$$\times \mathrm{i} \frac{\omega_\mathrm{p}^2 \boldsymbol{K}_0}{\boldsymbol{K}_0^2} \cdot \frac{\partial \varphi_a}{\partial \boldsymbol{v}_a} \int_0^{t-t_0-T_1} \mathrm{d}T_2 \, \mathrm{e}^{[-\mathrm{i}\boldsymbol{K}_0 \cdot \boldsymbol{v}_b (T_1-\tau_1)]} \int \mathrm{d}\boldsymbol{K}_1 \int \mathrm{d}\omega_1 \mathrm{i}\boldsymbol{F}_1(\omega_1, \boldsymbol{v}_\mathrm{p})$$

$$\times \mathrm{e}^{[-\mathrm{i}\omega_1 (t-T_1)]} \cdot \frac{\partial}{\partial \boldsymbol{v}_\mathrm{p}} \int_0^{T_2} \mathrm{d}\tau_2 \, \mathrm{e}^{[-\mathrm{i}(\boldsymbol{K}_1 \cdot \boldsymbol{v}_b + \boldsymbol{K}_1 \cdot \boldsymbol{v}_\mathrm{p})\tau_2]} \mathrm{i} \frac{\omega_\mathrm{p}^2 \boldsymbol{K}_0}{\boldsymbol{K}_0^2} \frac{\partial \varphi_b}{\partial \boldsymbol{v}_b}$$

$$\times \int_0^{T_2-\tau_2} \mathrm{d}\tau_3 \, \mathrm{e}^{[-\mathrm{i}(\boldsymbol{K}_c\cdot\boldsymbol{v}_c+\boldsymbol{K}_1\cdot\boldsymbol{v}_r)\tau_3]}\mathrm{i}\frac{\omega_p^2\boldsymbol{K}_1}{\boldsymbol{K}_i^2}\cdot\frac{\partial\varphi_r}{\partial\boldsymbol{v}_r}$$

$$\times \mathrm{e}^{[-\mathrm{i}\{\boldsymbol{K}_0\cdot\boldsymbol{v}_c+\boldsymbol{K}_1\cdot\boldsymbol{v}_q)(T_2-\tau_2-\tau_3)]}\int \mathrm{d}\omega_2 \mathrm{i}\boldsymbol{F}_1(\omega_2;\boldsymbol{v}_2)$$

$$\times \mathrm{e}^{[-\mathrm{i}\omega_2(t-T_1-T_2)]}\cdot\frac{\partial}{\partial\boldsymbol{v}_q}\int_0^{t-t_0-T_1-T_2}\mathrm{d}\tau_4\,\mathrm{e}^{(-\mathrm{i}\boldsymbol{K}_0\cdot\boldsymbol{v}_c\tau_4)}$$

$$\times \mathrm{i}\frac{\omega_p^2\boldsymbol{K}_0}{\boldsymbol{K}_0^2}\frac{\partial\varphi_c}{\partial\boldsymbol{v}_c}\mathrm{e}^{[-\mathrm{i}\boldsymbol{K}_0\cdot\boldsymbol{v}_d(t-t_0-T_1-T_2-\tau_4)]}f_{\boldsymbol{K}_0}(\boldsymbol{v}_d;t_0) \tag{3.1}$$

can be computed using the methods developed in I. For the choice of first level subdynamics shown in this figure (labelled by dotted single vertical lines), we have

$$h_{\boldsymbol{K}_{0a}}(t)\doteq\int \mathrm{d}\Gamma\frac{1}{\mathrm{i}\xi-\boldsymbol{K}_0\cdot\boldsymbol{v}_{ab}}\mathscr{V}_{0a}\int_0^{t-t_0}\mathrm{d}T_1\,\mathrm{e}^{[\mathrm{i}(\omega_{12}-\boldsymbol{K}_0\cdot\boldsymbol{v}_{bd})T_1]}\boldsymbol{F}_{1r}\cdot\frac{\partial}{\partial\boldsymbol{v}_r}$$

$$\times\frac{1}{\mathrm{i}\xi-\boldsymbol{K}_0\cdot\boldsymbol{v}_{bc}-\boldsymbol{K}_1\cdot\boldsymbol{v}_{rq}}\mathscr{V}_{kb}\frac{1}{\mathrm{i}\xi-\boldsymbol{K}_1\cdot\boldsymbol{v}_{rq}}\mathscr{V}_{1r}\int_0^{t-t_0-T_1}\mathrm{d}T_2$$

$$\times\mathrm{e}^{[\mathrm{i}(\omega_2-\boldsymbol{K}_0\cdot\boldsymbol{v}_{cd}-\boldsymbol{K}_1\cdot\boldsymbol{v}_q)]}\boldsymbol{F}_{1q}\cdot\frac{\partial}{\partial\boldsymbol{v}_q}$$

$$\times\frac{1}{\mathrm{i}\xi-\boldsymbol{K}_0\cdot\boldsymbol{v}_{cd}}\mathscr{V}_{0c}\,\mathrm{e}^{[-\mathrm{i}\boldsymbol{K}_0\cdot\boldsymbol{v}_d(t-t_0)]}f_{\boldsymbol{K}_0}(\boldsymbol{v}_d;t_0) \tag{3.2}$$

where the notation is the same as that employed in I. The contribution to the generalised subdynamics (two vertical dotted lines in figure 3(a)), which always coincides with the first-level subdynamics lying furthest to the right in the diagram, is then calculated:

$$h_{\boldsymbol{K}_{0a}}(t)\doteq\int \mathrm{d}\Gamma\frac{1}{\mathrm{i}\xi-\boldsymbol{K}_1\cdot\boldsymbol{v}_{ab}}\mathscr{V}_{0a}\frac{1}{\mathrm{i}\xi-\boldsymbol{K}_0\cdot\boldsymbol{v}_b+\boldsymbol{K}_0\cdot\boldsymbol{v}_d+\omega_{12}}\boldsymbol{F}_{1r}\cdot\frac{\partial}{\partial\boldsymbol{v}_r}$$

$$\times\frac{1}{\mathrm{i}\xi-\boldsymbol{K}_0\cdot\boldsymbol{v}_{bc}-\boldsymbol{K}_1\cdot\boldsymbol{v}_{rq}}\mathscr{V}_{0b}\frac{1}{\mathrm{i}\xi-\boldsymbol{K}_1\cdot\boldsymbol{v}_{rq}}\mathscr{V}_{1p}$$

$$\frac{1}{\mathrm{i}\xi-\boldsymbol{K}_0\cdot\boldsymbol{v}_c-\boldsymbol{K}_1\cdot\boldsymbol{v}_q+\boldsymbol{K}_0\cdot\boldsymbol{v}_d+\omega_2}$$

$$\times\boldsymbol{F}_{1q}\cdot\frac{\partial}{\partial\boldsymbol{v}_q}\frac{1}{\mathrm{i}\xi-\boldsymbol{K}_0\cdot\boldsymbol{v}_{cd}}\mathscr{V}_{0c}\,\mathrm{e}^{[-\mathrm{i}\boldsymbol{K}_0\cdot\boldsymbol{v}_d(t-t_0)]}f_{\boldsymbol{K}_0}(\boldsymbol{v}_d;t_0). \tag{3.3}$$

Inspection of (3.1) reveals that the particles labelling the two separate lines are nevertheless *mixed* in the propagator corresponding to that part of the diagram.

To obtain the solution of the Vlasov equation we must sum the contributions from the whole family of diagrams $\{V\}$ (figure 2 of I). It will be recalled that the diagrams in this family differ only in the number of loop vertices. In I, it was shown that, for one-line diagrams, a propagator with a loop on its right contributes an independent integral J (equation (3.7) of I) over the velocity of the particle concerned, provided that this propagator is not associated with either a subdynamics (i.e. S_0, S_1 and E in figure 3(a)) or the domain of an EF vertex (e.g. F_1). Furthermore, when the whole family of diagrams is taken, these J-terms form the sum of a geometrical progression which is nothing other than the reciprocal of the plasma dielectric function ε.

However, in the present situation involving two lines, the mixing of the particles which occurs in the propagator inhibits the isolation of a single J-integral. Fortunately, this difficulty can be circumvented by using the property of 'dynamical factorisation' which has been established elsewhere (Škarka 1987a, b, 1989a, b). This property applies to both diagrams and parts of diagrams which can be split by a horizontal line into two or more separate 'blocks'. A block does not contain any particle occurring in any other block (see, e.g., Škarka and Coveney 1988). Consequently, each block contributes a dynamically independent term to a subdynamics: it is as if each block were a completely separate diagram.

In order to factorise the contributions coming from two blocks within a diagram, we must consider the whole *permutation class* of such diagrams. This class is obtained from a given diagram by keeping the same time ordering of IF vertices in each block but taking all possible permutations of the mutual ordering of the vertices between different blocks in such a way that the vertices belonging to a given subdynamics remain within that subdynamics. This restriction arises by virtue of the presence of more than one (first level) subdynamics, in contradistinction with the case of only one which was treated previously (Škarka 1987a, b, 1989a, b).

For example, the diagram in figure 3(a) contains two lines and therefore two blocks; by shifting one loop vertex with respect to the other while keeping the same time ordering in each block and all subdynamics unchanged, we obtain figure 3(b). In this diagram, two loops in the central subdynamics are interchanged relative to figure 3(a). The corresponding contribution of figure 3(b) is

$$h_{\boldsymbol{K}_{0a}}(t) \doteq \int \mathrm{d}\Gamma \frac{1}{\mathrm{i}\xi - \boldsymbol{K}_0 \cdot \boldsymbol{v}_{ab}} \mathscr{V}_{0a} \frac{1}{\mathrm{i}\xi - \boldsymbol{K}_0 \cdot \boldsymbol{v}_b + \boldsymbol{K}_0 \cdot \boldsymbol{v}_d + \omega_{12}} \boldsymbol{F}_{1r} \cdot \frac{\partial}{\partial \boldsymbol{v}_r}$$
$$\times \frac{1}{\mathrm{i}\xi - \boldsymbol{K}_0 \cdot \boldsymbol{v}_{bc} - \boldsymbol{v}_{rq}} \mathscr{V}_{1r} \frac{1}{\mathrm{i}\xi - \boldsymbol{K}_0 \cdot \boldsymbol{v}_{bc}} \mathscr{V}_{0b} \frac{1}{\mathrm{i}\xi - \boldsymbol{K}_0 \cdot \boldsymbol{v}_c - \boldsymbol{K}_1 \cdot \boldsymbol{v}_q + \boldsymbol{K}_0 \cdot \boldsymbol{v}_d + \omega_2}$$
$$\times \boldsymbol{F}_{1q} \cdot \frac{\partial}{\partial \boldsymbol{v}_q} \frac{1}{\mathrm{i}\xi - \boldsymbol{K}_0 \cdot \boldsymbol{v}_{cd}} \mathscr{V}_{0c} \, \mathrm{e}^{[-\mathrm{i}\boldsymbol{K}_0 \cdot \boldsymbol{v}_d (t - t_0)]} f_{\boldsymbol{K}_0}(\boldsymbol{v}_d; t_0). \tag{3.4}$$

By means of the relation

$$\lim_{\xi \to 0} \frac{1}{\mathrm{i}\xi + a + b} \left(\frac{1}{\mathrm{i}\xi + a} + \frac{1}{\mathrm{i}\xi + b} \right) = \lim_{\xi \to 0} \frac{1}{\mathrm{i}\xi + a} \frac{1}{\mathrm{i}\xi + b} \tag{3.5}$$

which is a consequence of the Poincaré-Bertrand theorem for Schwartz distributions (Balescu 1963, George 1970), we can sum (3.3) and (3.4)

$$h_{\boldsymbol{K}_{0a}}(t) \doteq \int \mathrm{d}\Gamma \frac{1}{\mathrm{i}\xi - \boldsymbol{K}_0 \cdot \boldsymbol{v}_{ab}} \mathscr{V}_{0a} \frac{1}{\mathrm{i}\xi - \boldsymbol{K}_0 \cdot \boldsymbol{v}_b + \boldsymbol{K}_0 \cdot \boldsymbol{v}_d + \omega_{12}} \boldsymbol{F}_{1r} \cdot \frac{\partial}{\partial \boldsymbol{v}_r}$$
$$\times \frac{1}{\mathrm{i}\xi - \boldsymbol{K}_1 \cdot \boldsymbol{v}_{rq}} \mathscr{V}_{1r} \frac{1}{\mathrm{i}\xi - \boldsymbol{K}_0 \cdot \boldsymbol{v}_{bc}} \mathscr{V}_{0b} \frac{1}{\mathrm{i}\xi - \boldsymbol{K}_0 \cdot \boldsymbol{v}_c - \boldsymbol{K}_1 \cdot \boldsymbol{v}_q + \boldsymbol{K}_0 \cdot \boldsymbol{v}_d + \omega_2}$$
$$\times \boldsymbol{F}_{1q} \cdot \frac{\partial}{\partial \boldsymbol{v}_q} \frac{1}{\mathrm{i}\xi - \boldsymbol{K}_0 \cdot \boldsymbol{v}_{cd}} \mathscr{V}_{0c} \exp[-\mathrm{i}\boldsymbol{K}_0 \cdot \boldsymbol{v}_d (t - t_0)] f_{\boldsymbol{K}_0}(\boldsymbol{v}_d; t_0). \tag{3.6}$$

The two-line part of the diagram between the two EF vertices is now seen to be dynamically factorised, contributing two mutually independent terms which come from the two blocks. The exception is the propagator associated with the subdynamics itself which remains unfactorised, but this presents no problems because it does not contribute through J to the dielectric function.

As in previous cases described in I, the propagators immediately before and after an EF vertex (F_1 etc) do not give rise to any J terms. However, this is also true for propagators associated with the upper line, even though this line does not contain any EF vertices. Therefore, in the present case there are no J terms. The reason is that each EF vertex on the lower line marks the division between different first-level subdynamics. Thus the propagator on the upper line is cut into two parts by the presence of an EF vertex on the lower line; each part belongs to a separate subdynamics. This is why there are two distinct propagators with the same particle index (b) distinguished only by their different subdynamics indices.

If the overlapping part of a two-line diagram contains three loops, there are instead three diagrams in the permutation class (because there are three possible permutations of the mutual ordering of these loops). They are represented in figure 4 using arrows to depict all possible permutations of the loop vertex in the second block with respect to those in the first one. The diagrams in this case can be summed using (3.5) twice

$$\begin{aligned} h_{\boldsymbol{K}_{0a}}(t) \doteq \int \mathrm{d}\Gamma' & \frac{1}{\mathrm{i}\xi - \boldsymbol{K}_0 \cdot \boldsymbol{v}_{ab}} \mathscr{V}_{0a} \frac{1}{\mathrm{i}\xi - \boldsymbol{K}_0 \cdot \boldsymbol{v}_{bd} + \omega_{12}} \boldsymbol{F}_{1r} \cdot \frac{\partial}{\partial \boldsymbol{v}_r} \\ & \times \frac{1}{\mathrm{i}\xi - \boldsymbol{K}_1 \cdot \boldsymbol{v}_{rq}} \mathscr{V}_{1r} \frac{1}{\mathrm{i}\xi - \boldsymbol{K}_0 \cdot \boldsymbol{v}_{bc}} \mathscr{V}_{0b} \left\{ \int \mathrm{d}\boldsymbol{v}_e \frac{1}{\mathrm{i}\xi - \boldsymbol{K}_0 \cdot \boldsymbol{v}_{ec}} \mathscr{V}_{0e} \right\} \\ & \times \frac{1}{\mathrm{i}\xi - \boldsymbol{K}_0 \cdot \boldsymbol{v}_{cd} - \boldsymbol{K}_1 \cdot \boldsymbol{v}_q + \omega_2} \boldsymbol{F}_{1q} \cdot \frac{\partial}{\partial \boldsymbol{v}_q} \frac{1}{\mathrm{i}\xi - \boldsymbol{K}_0 \cdot \boldsymbol{v}_{cd}} \mathscr{V}_{0c} \\ & \times \mathrm{e}^{[-\mathrm{i}\boldsymbol{K}_0 \cdot \boldsymbol{v}_d (t - t_0)]} f_{\boldsymbol{K}_0}(\boldsymbol{v}_d; t_0) \end{aligned} \tag{3.7}$$

where we recognise one J term (in braces) depending only on the indices labelling the upper block.

The procedure can evidently be carried out for arbitrarily many loop vertices by repeated application of (3.5). Indeed it has been shown elsewhere (Škarka 1989b) that the property of dynamical factorisation holds for arbitrary order in the coupling constant.

It follows that the sum of the whole family $\{V\}$ of diagrams (drawn in figure 5 with the corresponding choice of subdynamics) is given by summing first each permutation class and then over the J terms appearing in the dynamically factorised form:

$$\begin{aligned} h_{\boldsymbol{K}_{0\alpha}}(t) \doteq \int \mathrm{d}\Gamma & \frac{1}{\varepsilon(\boldsymbol{K}_0)} \frac{1}{\mathrm{i}\xi - \boldsymbol{K}_0 \cdot \boldsymbol{v}_\sigma + \boldsymbol{K}_0 \cdot \boldsymbol{v}_\Sigma + \omega_{yz}} \mathscr{V}_{0\sigma} \\ & \times \frac{1}{\varepsilon^{\mathrm{cc}}(\boldsymbol{K}_0)} \frac{1}{-\mathrm{i}\xi - \boldsymbol{K}_0 \cdot \boldsymbol{v}_{\beta\sigma}} \boldsymbol{F}_{1\eta} \cdot \frac{\partial}{\partial \boldsymbol{v}_\eta} \frac{1}{\mathrm{i}\xi - \boldsymbol{K}_0 \cdot \boldsymbol{v}_{\gamma\Sigma} - \boldsymbol{K}_1 \cdot \boldsymbol{v}_\mu + \omega_z} \\ & \times \frac{1}{\mathrm{i}\xi - \boldsymbol{K}_0 \cdot \boldsymbol{v}_{\beta\gamma}} \mathscr{V}_{0\beta} \frac{1}{\varepsilon(\boldsymbol{K}_0)} \mathscr{V}_{0\gamma} \frac{1}{\varepsilon^{\mathrm{cc}}(\boldsymbol{K}_0)} \frac{1}{-\mathrm{i}\xi - \boldsymbol{K}_0 \cdot \boldsymbol{v}_{\chi\gamma}} \\ & \frac{1}{\mathrm{i}\xi - \boldsymbol{K}_1 \cdot \boldsymbol{v}_{\eta\mu}} \mathscr{V}_{1\eta} \frac{1}{\varepsilon(\boldsymbol{K}_1)} \mathscr{V}_{1\mu} \frac{1}{\varepsilon^{\mathrm{cc}}(\boldsymbol{K}_1)} \frac{1}{-\mathrm{i}\xi - \boldsymbol{K}_1 \cdot \boldsymbol{v}_{\nu\mu}} \boldsymbol{F}_{2\nu} \cdot \frac{\partial}{\partial \boldsymbol{v}_\nu} \\ & \times \frac{1}{\mathrm{i}\xi - \boldsymbol{K}_0 \cdot \boldsymbol{v}_{\chi\Sigma}} \mathscr{V}_{0\chi} \frac{1}{\varepsilon(\boldsymbol{K}_0)} \mathrm{e}^{[-\mathrm{i}\boldsymbol{K}_0 \cdot \boldsymbol{v}_\Sigma (t - t_0)]} \mathscr{V}_{0\Sigma} \\ & \times \frac{1}{\varepsilon^{\mathrm{cc}}(\boldsymbol{K}_0)} \frac{1}{-\mathrm{i}\xi - \boldsymbol{K}_0 \cdot \boldsymbol{v}_{\rho\Sigma}} f_{\boldsymbol{K}_0}(\boldsymbol{v}_\rho; t_0). \end{aligned} \tag{3.8}$$

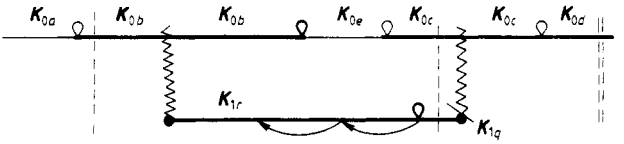

Figure 4. A diagram in the class $\{Q\}$. The arrows represent displacements of a single loop vertex which generate the permutation class associated with this diagram.

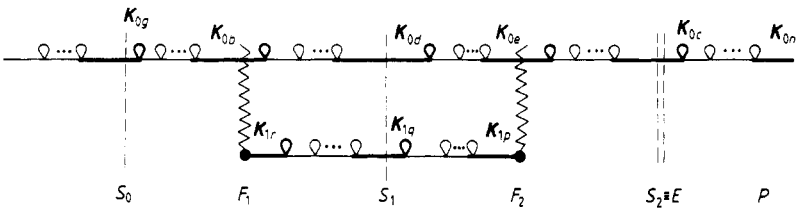

Figure 5. The sum of the complete class $\{Q\}$ of diagrams for the particular choice of subdynamics shown.

This general formula can now be used to write directly from the diagram an explicit expression for each possible choice of subdynamics. In order to obtain the sum over all subdynamics, the symbolic expression (2.5) is of great help for taking into account these different choices. Indeed, although (2.5) was originally constructed for single-line diagrams, it can also be applied to those with two lines, since the sequence of external field terms, dielectric constants, and subdynamical propagators is the same for all two-EF-vertex diagrams. However, in the two-line part of a diagram dielectric functions arise in pairs, each associated with a single line. Also, the convention for translating a symbolic expression into an explicit one by means of (3.8) is different when the corresponding diagram contains two lines. It is in fact simpler since, owing to the particular topology of two-block diagrams, even when we encounter the term F_E, we have to deal only with generalised subdynamics for which the subdynamical propagator E, residing in a different block, does not share a particle with the derivative from the vertex F_E. Consequently, there is no need to invert the ordering of any terms in explicit expressions compared to their appearance in the diagrams and symbolic formulae.

The combination of the results of sections 2 and 3 thus provide the complete solution of the linearised Vlasov equation up to second order with respect to the external field.

4. Higher-order contributions

We now move on to a consideration of the contributions to the solution of the Vlasov equation at third and higher orders with respect to the external field. These contributions can be readily worked out following the methods described hitherto. For this reason, we do not provide all the details of the calculations.

4.1. Contributions from single-line diagrams

We first discuss the case of single-line diagrams. One such third-order diagram is shown in figure 6. For the choice of subdynamics indicated in figure 6, we

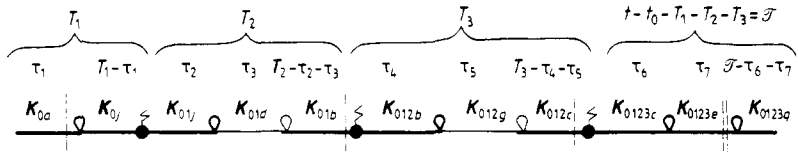

Figure 6. A particular diagram in the class $\{P\}$ of three external vertex diagrams.

get the expression

$$h_{\boldsymbol{K}_{0a}}(t) \doteq \int \mathrm{d}\Gamma \frac{1}{\mathrm{i}\xi+\omega_{123}-\boldsymbol{K}_0\cdot\boldsymbol{v}_a+\boldsymbol{K}_{0123}\cdot\boldsymbol{v}_e}\mathscr{V}_{0a}\frac{1}{-\mathrm{i}\xi-\boldsymbol{K}_0\cdot\boldsymbol{v}_{ja}}\boldsymbol{F}_{j1}\cdot\frac{\partial}{\partial\boldsymbol{v}_j}$$
$$\times\frac{1}{\mathrm{i}\xi-\boldsymbol{K}_{01}\cdot\boldsymbol{v}_{jb}}\mathscr{V}_{1j}\frac{1}{\mathrm{i}\xi-\boldsymbol{K}_{01}\cdot\boldsymbol{v}_{db}}\mathscr{V}_{1d}\frac{1}{\mathrm{i}\xi+\omega_{23}-\boldsymbol{K}_{01}\cdot\boldsymbol{v}_b+\boldsymbol{K}_{0123}\cdot\boldsymbol{v}_e}$$
$$\times\boldsymbol{F}_{2b}\cdot\frac{\partial}{\partial\boldsymbol{v}_b}\frac{1}{\mathrm{i}\xi-\boldsymbol{K}_{012}\cdot\boldsymbol{v}_{bc}}\mathscr{V}_{2b}\frac{1}{\mathrm{i}\xi-\boldsymbol{K}_{012}\cdot\boldsymbol{v}_{gc}}\mathscr{V}_{2g}$$
$$\times\frac{1}{\mathrm{i}\xi+\omega_3-\boldsymbol{K}_{012}\cdot\boldsymbol{v}_c+\boldsymbol{K}_{0123}\cdot\boldsymbol{v}_e}\boldsymbol{F}_{3c}\cdot\frac{\partial}{\partial\boldsymbol{v}_c}\frac{1}{\mathrm{i}\xi-\boldsymbol{K}_{0123}\cdot\boldsymbol{v}_{ce}}\mathscr{V}_{3c}$$
$$\times\mathrm{e}^{[-\mathrm{i}\boldsymbol{K}_{0123}\cdot\boldsymbol{v}_e(t-t_0)]}\mathscr{V}_{3e}\frac{1}{-\mathrm{i}\xi-\boldsymbol{K}_{0123}\cdot\boldsymbol{v}_{qe}}f_{\boldsymbol{K}_{0123}}(\boldsymbol{v}_q;\,t_0). \tag{4.1}$$

The class of diagrams with three EF vertices contains diagrams (like the one in figure 6) with all possible numbers of loops; it is represented in figure 7. The corresponding contribution of this class is computed in the usual way:

$$h_{\boldsymbol{K}_{0a}}(t) \doteq \int \mathrm{d}\Gamma \frac{1}{\varepsilon(\boldsymbol{K}_0)}\frac{1}{\mathrm{i}\xi-\boldsymbol{K}_0\cdot\boldsymbol{v}_g+\boldsymbol{K}_{0123}\cdot\boldsymbol{v}_c+\omega_{123}}\mathscr{V}_{0g}\frac{1}{\varepsilon^{\mathrm{cc}}(\boldsymbol{K}_0)}$$
$$\times\frac{1}{-\mathrm{i}\xi-\boldsymbol{K}_0\cdot\boldsymbol{v}_{bg}}\boldsymbol{F}_{1b}\cdot\frac{\partial}{\partial\boldsymbol{v}_b}\frac{1}{\mathrm{i}\xi-\boldsymbol{K}_{01}\cdot\boldsymbol{v}_{bd}}\mathscr{V}_{1b}\frac{1}{\varepsilon(\boldsymbol{K}_{01})}$$
$$\times\frac{1}{\mathrm{i}\xi-\boldsymbol{K}_{01}\cdot\boldsymbol{v}_d+\boldsymbol{K}_{0123}\cdot\boldsymbol{v}_c+\omega_{23}}\mathscr{V}_{1d}\frac{1}{\varepsilon^{\mathrm{cc}}(\boldsymbol{K}_{01})}\frac{1}{-\mathrm{i}\xi-\boldsymbol{K}_{01}\cdot\boldsymbol{v}_{ed}}$$
$$\times\boldsymbol{F}_{2e}\cdot\frac{\partial}{\partial\boldsymbol{v}_e}\frac{1}{\mathrm{i}\xi-\boldsymbol{K}_{012}\cdot\boldsymbol{v}_{ej}}\mathscr{V}_{2e}\frac{1}{\varepsilon(\boldsymbol{K}_{012})}$$
$$\times\frac{1}{\mathrm{i}\xi-\boldsymbol{K}_{012}\cdot\boldsymbol{v}_j+\boldsymbol{K}_{0123}\cdot\boldsymbol{v}_c+\omega_3}\mathscr{V}_{2j}\frac{1}{\varepsilon^{\mathrm{cc}}(\boldsymbol{K}_{012})}$$
$$\times\frac{1}{-\mathrm{i}\xi-\boldsymbol{K}_{012}\cdot\boldsymbol{v}_{qj}}\boldsymbol{F}_{3q}\cdot\frac{\partial}{\partial\boldsymbol{v}_q}\frac{1}{\mathrm{i}\xi-\boldsymbol{K}_{0123}\cdot\boldsymbol{v}_{qc}}\mathscr{V}_{3q}\frac{1}{\varepsilon(\boldsymbol{K}_{0123})}$$
$$\times\mathrm{e}^{[-\mathrm{i}\boldsymbol{K}_{0123}\cdot\boldsymbol{v}_c(t-t_0)]}\mathscr{V}_{3c}\frac{1}{\varepsilon^{\mathrm{cc}}(\boldsymbol{K}_{0123})}\frac{1}{-\mathrm{i}\xi-\boldsymbol{K}_{0123}\cdot\boldsymbol{v}_{pc}}f_{\boldsymbol{K}_{0123}}(\boldsymbol{v}_p;\,t_0). \tag{4.2}$$

Figure 7. The class $\{P\}$ of three EF vertex diagrams.

By analysing this expression in association with (2.3) and equations (4.21) and (4.26) from I, one notices a general structure based on the repetition of the single EF vertex pattern. The only non-trivial modification concerns the appearance of a frequency sum in the denominator of the propagator S_i, corresponding to the frequencies associated with all the EF vertices appearing between this first level subdynamics propagator and the generalised subdynamics one, E. For these reasons, it is possible to deduce a general formula for the contribution from the class $\{P\}$ of diagrams of arbitrary order (see figure 2 in I), along the same lines as was done in I and section 2 above. We obtain the following general expression:

$$
\begin{aligned}
h_{\boldsymbol{K}_{M\alpha}}(t) \doteq \int \mathrm{d}\Gamma\, & \frac{1}{\varepsilon(\boldsymbol{K}_M)}\,\frac{1}{\mathrm{i}\xi - \boldsymbol{K}_M\cdot\boldsymbol{v}_\mu + \boldsymbol{K}_{M\ldots z}\cdot\boldsymbol{v}_\Sigma + \omega_{N\ldots z}}\,\mathscr{V}_{M\mu} \\
& \times \frac{1}{\varepsilon^{\mathrm{cc}}(\boldsymbol{K}_M)}\,\frac{1}{-\mathrm{i}\xi - \boldsymbol{K}_M\cdot\boldsymbol{v}_{\beta\mu}}\,\boldsymbol{F}_{N\beta}\cdot\frac{\partial}{\partial\boldsymbol{v}_\beta}\,\frac{1}{\mathrm{i}\xi - \boldsymbol{K}_{MN}\cdot\boldsymbol{v}_{\beta\eta}}\,\mathscr{V}_{N\beta}\,\frac{1}{\varepsilon(\boldsymbol{K}_{MN})} \\
& \times \frac{1}{\mathrm{i}\xi - \boldsymbol{K}_{MN}\cdot\boldsymbol{v}_\eta + \boldsymbol{K}_{M\ldots z}\cdot\boldsymbol{v}_\Sigma + \omega_{0\ldots z}}\,\mathscr{V}_{M\eta}\,\frac{1}{\varepsilon^{\mathrm{cc}}(\boldsymbol{K}_{MN})} \\
& \times \frac{1}{-\mathrm{i}\xi - \boldsymbol{K}_{MN}\cdot\boldsymbol{v}_{\gamma\eta}}\,\boldsymbol{F}_{0\gamma}\cdot\frac{\partial}{\partial\boldsymbol{v}_\gamma}\,\frac{1}{\mathrm{i}\xi - \boldsymbol{K}_{MN0}\cdot\boldsymbol{v}_{\gamma\omega}}\,\mathscr{V}_{0\gamma}\,\frac{1}{\varepsilon(\boldsymbol{K}_{MN0})} \\
& \times \frac{1}{\mathrm{i}\xi - \boldsymbol{K}_{MN0}\cdot\boldsymbol{v}_\omega + \boldsymbol{K}_{M\ldots z}\cdot\boldsymbol{v}_\Sigma + \omega_{p\ldots z}}\,\mathscr{V}_{0\omega}\ldots\boldsymbol{F}_{y\nu}\cdot\frac{\partial}{\partial\boldsymbol{v}_\nu} \\
& \times \frac{1}{\mathrm{i}\xi - \boldsymbol{K}_{M\ldots y}\cdot\boldsymbol{v}_{\nu\sigma}}\,\mathscr{V}_{y\nu}\,\frac{1}{\varepsilon(\boldsymbol{K}_{M\ldots y})}\,\frac{1}{\mathrm{i}\xi - \boldsymbol{K}_{M\ldots y}\cdot\boldsymbol{v}_\sigma + \boldsymbol{K}_{M\ldots z}\cdot\boldsymbol{v}_\Sigma + \omega_z}\,\mathscr{V}_{y\sigma} \\
& \times \frac{1}{\varepsilon^{\mathrm{cc}}(\boldsymbol{K}_{M\ldots y})}\,\frac{1}{-\mathrm{i}\xi - \boldsymbol{K}_{M\ldots y}\cdot\boldsymbol{v}_{\zeta\sigma}}\,\boldsymbol{F}_{z\zeta}\cdot\frac{\partial}{\partial\boldsymbol{v}_\zeta}\,\frac{1}{\mathrm{i}\xi - \boldsymbol{K}_{M\ldots z}\cdot\boldsymbol{v}_{\zeta\Sigma}}\,\mathscr{V}_{z\zeta} \\
& \times \frac{1}{\varepsilon(\boldsymbol{K}_{M\ldots z})}\,\mathrm{e}^{[-\mathrm{i}\boldsymbol{K}_{M\ldots z}\cdot\boldsymbol{v}_\Sigma(t-t_0)]}\mathscr{V}_{z\Sigma}\,\frac{1}{\varepsilon^{\mathrm{cc}}(\boldsymbol{K}_{M\ldots z})} \\
& \times \frac{1}{-\mathrm{i}\xi - \boldsymbol{K}_{M\ldots z}\cdot\boldsymbol{v}_{\chi\Sigma}}\,f_{\boldsymbol{K}_{M\ldots z}}(\boldsymbol{v}_\chi;\, t_0). \qquad (4.3)
\end{aligned}
$$

As before, the contribution of a given diagram for a particular choice of subdynamics can be obtained from this formula by replacing all wavevector and particle indices in (4.3) by concrete ones read from that diagram.

Equations (4.2) and (4.3) describe the most general situation when the subdynamics are chosen in such a way that the propagators associated with them (denoted S_i following the conventions of I) never coincide with the propagators immediately before and after the EF vertex (labelled F_y). If they do coincide there are no IF (loop) vertices between them and in this case the corresponding plasma dielectric function or $(1/\varepsilon)$-

term in (4.3) must be omitted. There are respectively four and sixteen such combinations for diagrams with one and two EF vertices; all of them have been previously enumerated and their contributions computed in I and section 2 above. When each new EF vertex is added the number of such possible combinations is multiplied by four. Since the solution of the Vlasov equation is given in terms of a sum over all subdynamics, at third order we must sum sixty-four distinct cases. As before, this can be done symbolically by utilising the notation introduced in I:

$$\frac{1}{\varepsilon}\left[\left[\left(s_0F+S_0\frac{1}{\varepsilon^{cc}}F\right)\frac{1}{\varepsilon}\left\{\left(s_1F+S_1\frac{1}{\varepsilon^{cc}}F\right)\frac{1}{\varepsilon}\left[\left(s_2F+S_2\frac{1}{\varepsilon^{cc}}F\right)\frac{1}{\varepsilon}E+s_2F_E+S_2\frac{1}{\varepsilon^{cc}}F_E\right]\right.\right.\right.$$
$$\left.+\left(s_1F_{s_2}+S_1\frac{1}{\varepsilon^{cc}}F_{s_2}\right)\left[\frac{1}{\varepsilon^{cc}}\left(F_E+F\frac{1}{\varepsilon}E\right)+s_2F_E+s_2F\frac{1}{\varepsilon}E\right]\right\}$$
$$+\left(s_0F_{s_1}+S_0\frac{1}{\varepsilon^{cc}}F_{s_1}\right)\left\{\left(\frac{1}{\varepsilon^{cc}}F+s_1F\right)\frac{1}{\varepsilon}\left[\left(s_2F+S_2\frac{1}{\varepsilon^{cc}}F\right)\frac{1}{\varepsilon}E\right.\right.$$
$$\left.+s_2F_E+S_2\frac{1}{\varepsilon^{cc}}F_E\right]+\left(s_1F_{s_2}+\frac{1}{\varepsilon^{cc}}F_{s_2}\right)$$
$$\left.\left.+\left[\frac{1}{\varepsilon^{cc}}\left(F_E+F\frac{1}{\varepsilon}E\right)+s_2F_E+s_2F\frac{1}{\varepsilon}E\right]\right\}\right]\frac{1}{\varepsilon^{cc}}P. \tag{4.4}$$

As in section 2, in order to write all these contributions explicitly, the general formula (4.3) (specifically its third-order part) has to be applied together with (4.4). Since all EF vertices lie on the same line, the convention inverting the order of appearance of the propagators S_i relative to the F_E-terms in the algebraic expressions, established in I and reiterated in section 2, has to be applied.

In an analogous fashion, explicit higher-order expressions can be generated using (4.3) up to arbitrary order.

4.2. Contributions from two-line diagrams

When we come to consider the third-order contribution from two-line diagrams (figure 8) (from the class $\{W\}$ in figure 2 of I), the situation is very similar to that described in section 3 for second-order contributions.

In figure 8 we give as an example only the simplest permutation class (as before, an arrow indicates the corresponding permutation of loop vertices). The dynamical factorisation of the contributions coming from different blocks is obtained using (3.5)

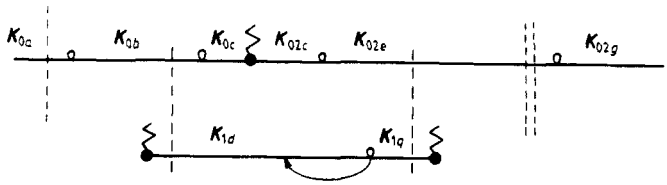

Figure 8. A particular diagram in the class $\{W\}$. The arrow indicates the permutation of loop vertices.

as before

$$h_{\boldsymbol{K}_{0a}}(t) \doteq \int \mathrm{d}\Gamma \frac{1}{\mathrm{i}\xi - \boldsymbol{K}_0 \cdot \boldsymbol{v}_a + \boldsymbol{K}_{02} \cdot \boldsymbol{v}_e + \omega_{123}} \mathscr{V}_{0a} \frac{1}{-\mathrm{i}\xi - \boldsymbol{K}_0 \cdot \boldsymbol{v}_{ba}} \boldsymbol{F}_{1r} \cdot \frac{\partial}{\partial \boldsymbol{v}_r}$$
$$\times \frac{1}{\mathrm{i}\xi - \boldsymbol{K}_0 \cdot \boldsymbol{v}_b - \boldsymbol{K}_1 \cdot \boldsymbol{v}_d + \boldsymbol{K}_{02} \cdot \boldsymbol{v}_e + \omega_{23}} \mathscr{V}_{0b} \frac{1}{-\mathrm{i}\xi - \boldsymbol{K}_0 \cdot \boldsymbol{v}_{cb}} \boldsymbol{F}_{2c} \cdot \frac{\partial}{\partial \boldsymbol{v}_c}$$
$$\times \frac{1}{\mathrm{i}\xi - \boldsymbol{K}_{02} \cdot \boldsymbol{v}_{ce}} \mathscr{V}_{2c} \frac{1}{\mathrm{i}\xi - \boldsymbol{K}_1 \cdot \boldsymbol{v}_{dq}} \mathscr{V}_{1d} \frac{1}{\mathrm{i}\xi - \boldsymbol{K}_1 \cdot \boldsymbol{v}_q + \omega_3} \boldsymbol{F}_{1q} \cdot \frac{\partial}{\partial \boldsymbol{v}_q}$$
$$\times \mathrm{e}^{[-\mathrm{i}\boldsymbol{K}_{02} \cdot \boldsymbol{v}_e (t - t_0)]} \mathscr{V}_{2e} \frac{1}{-\mathrm{i}\xi - \boldsymbol{K}_{02} \cdot \boldsymbol{v}_{ge}} f_{\boldsymbol{K}_{02}}(\boldsymbol{v}_g; t_0). \tag{4.5}$$

Note that now an EF vertex on the upper line cuts the propagator below on the lower line into two parts, each belonging to a separate subdynamics. This propagator is evidently a component of the EF term; hence, it does not contribute to a J quantity, for the reasons already explained in section 3.

We now represent in figure 9 the whole class $\{W\}$ of diagrams (see also figure 2 of I).

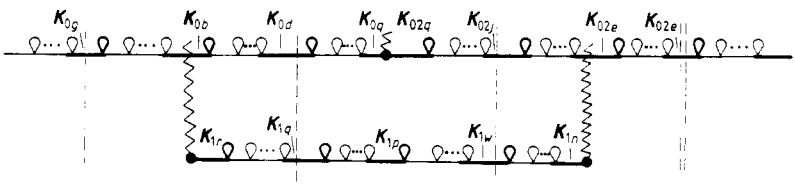

Figure 9. The complete class $\{W\}$ of two-line, three-EF-vertex diagrams.

Following the same procedure as in section 3, we write the general formula corresponding to this class of diagrams:

$$h_{\boldsymbol{K}_{x\alpha}}(t) \doteq \int \mathrm{d}\Gamma \frac{1}{\varepsilon(\boldsymbol{K}_x)} \frac{1}{\mathrm{i}\xi - \boldsymbol{K}_x \cdot \boldsymbol{v}_\sigma + \boldsymbol{K}_{xz} \cdot \boldsymbol{v}_\Sigma + \omega_{xyz}} \mathscr{V}_{x\sigma} \frac{1}{\varepsilon^{\mathrm{cc}}(\boldsymbol{K}_x)}$$
$$\times \frac{1}{-\mathrm{i}\xi - \boldsymbol{K}_x \cdot \boldsymbol{v}_{\beta\sigma}} \boldsymbol{F}_{y\eta} \cdot \frac{\partial}{\partial \boldsymbol{v}_\eta} \frac{1}{\mathrm{i}\xi - \boldsymbol{K}_x \cdot \boldsymbol{v}_\gamma - \boldsymbol{K}_y \cdot \boldsymbol{v}_\mu + \boldsymbol{K}_{xz} \cdot \boldsymbol{v}_\Sigma + \omega_{yz}}$$
$$\times \frac{1}{\mathrm{i}\xi - \boldsymbol{K}_x \cdot \boldsymbol{v}_{\beta\gamma}} \mathscr{V}_{x\beta} \frac{1}{\varepsilon(\boldsymbol{K}_x)} \mathscr{V}_{x\gamma} \frac{1}{\varepsilon^{\mathrm{cc}}(\boldsymbol{K}_x)} \frac{1}{-\mathrm{i}\xi - \boldsymbol{K}_x \cdot \boldsymbol{v}_{x\gamma}}$$
$$\times \frac{1}{\mathrm{i}\xi - \boldsymbol{K}_y \cdot \boldsymbol{v}_{\eta\mu}} \mathscr{V}_{y\eta} \frac{1}{\varepsilon(\boldsymbol{K}_y)} \mathscr{V}_{y\mu} \frac{1}{\varepsilon^{\mathrm{cc}}(\boldsymbol{K}_y)} \frac{1}{-\mathrm{i}\xi - \boldsymbol{K}_y \cdot \boldsymbol{v}_{\nu\mu}}$$
$$\times \boldsymbol{F}_{2\chi} \cdot \frac{\partial}{\partial \boldsymbol{v}_\chi} \frac{1}{\mathrm{i}\xi - \boldsymbol{K}_{xz} \cdot \boldsymbol{v}_{\pi\Sigma} - \boldsymbol{K}_y \cdot \boldsymbol{v}_\psi + \omega_z} \frac{1}{\mathrm{i}\xi - \boldsymbol{K}_{xz} \cdot \boldsymbol{v}_{\phi\pi}} \mathscr{V}_{z\phi}$$
$$\times \frac{1}{\varepsilon(\boldsymbol{K}_z)} \mathscr{V}_{z\pi} \frac{1}{\varepsilon^{\mathrm{cc}}(\boldsymbol{K}_z)} \frac{1}{-\mathrm{i}\xi - \boldsymbol{K}_z \cdot \boldsymbol{v}_{\Gamma\pi}} \frac{1}{\mathrm{i}\xi - \boldsymbol{K}_y \cdot \boldsymbol{v}_{\nu\psi}} \mathscr{V}_{y\Omega}$$

$$\times \frac{1}{\varepsilon(\boldsymbol{K}_\nu)} \mathscr{V}_{\nu\psi} \frac{1}{\varepsilon^{cc}(\boldsymbol{K}_\nu)} \frac{1}{-i\xi - \boldsymbol{K}_\nu \cdot \boldsymbol{v}_{\delta\psi}} \boldsymbol{F}_{1\delta} \cdot \frac{\partial}{\partial \boldsymbol{v}_\delta}$$

$$\times \frac{1}{i\xi - \boldsymbol{K}_z \cdot \boldsymbol{v}_{\Gamma\Sigma}} \mathscr{V}_{z\Gamma} \frac{1}{\varepsilon(\boldsymbol{K}_z)} e^{[-i\boldsymbol{K}_{xz} \cdot \boldsymbol{v}_\Sigma (t-t_0)]} \mathscr{V}_{z\Sigma}$$

$$\times \frac{1}{\varepsilon^{cc}(\boldsymbol{K}_z)} \frac{1}{-i\xi - \boldsymbol{K}_z \cdot \boldsymbol{v}_{\rho\Sigma}} f_{\boldsymbol{K}_{xz}}(\boldsymbol{v}_\rho; t_0). \tag{4.6}$$

This general expression can be extended to higher orders in a straightforward way, as has been done in the preceding subsection (section 4.1) for one-line diagrams.

The symbolic expression (4.4) enumerating all possible choices of subdynamics is the same for all third-order diagrams, regardless of the number of blocks they possess. Therefore, using this relation, the general formula (4.6), together with our algorithm, we can immediately write down the contributions from the family of diagrams $\{W\}$ to the solution of the Vlasov equation for all subdynamics.

For higher orders, the analysis proceeds in an exactly similar way. Then we encounter diagrams consisting of an arbitrary number of lines. No new principles emerge, however, since the dynamical factorisation procedure can be applied to multiblock diagrams by first separating the particles coming from a pair of blocks, and then separating these from those particles attached to other blocks (Škarka 1989b). Repeated application of (3.5) to the sum of the permutation class of these diagrams then provides the requisite dynamically factorised expression.

By this stage, we hope to have convinced the reader that there is a regular structure to the contributions arising order by order in the external field, and that it is a straightforward matter to compute the solution to the linearised Vlasov equation in the presence of an external field by this method.

Indeed, we would like to point out again (see I) that the subdynamics approach to the solution of kinetic equations is quite general and is not restricted to the treatment of the Vlasov equation alone.

5. Conclusions

In the present paper and the preceding one (I), we have obtained the solution of the linearised Vlasov equation describing a collisionless plasma evolving in an external field of arbitrary spatial and time dependence. We used statistical mechanical perturbation theory combined with diagrammatic techniques to develop a solution in powers of the external field. However, the solution includes *all* orders with respect to the internal interactions, in order to deal with collective effects arising from the long-range Coulomb interactions in a plasma.

In I, the solution was given to first order in the external field, while in the present article the analysis was extended to include higher orders. Beyond first order, some new features emerge which are associated with the presence of more than a single line in the diagrammatic representation. However, we have shown that it is still possible to find a regular structure in the contributions from higher orders. This permits us to write symbolic expressions directly from the diagrams while retaining the same ordering of sequences of terms. Using the conventions established in I, such symbolic formulae can be translated into algebraic expressions: these are in turn rendered fully explicit on insertion of specific particle and wavevector indices pertaining to any given family

of diagrams. Thus these contributions, like those in first order, can be computed by means of a simple algorithm which is very convenient for implementation using symbolic computation techniques. This is of considerable importance for future concrete applications of our approach.

In the context of laser-plasma interactions, there is a real need for analytical techniques which will cater, at one and the same time, for plasmas which are both non-Maxwellian and strongly inhomogeneous. Our approach, which is complementary to existing particle-simulation and other numerical methods, represents a new, microscopically based kinetic theory that may be able to provide fresh insight into some of these processes.

Acknowledgments

We are grateful to Professor R Balescu, Professor C George, and Dr H C Barr for helpful discussions, and to Professor I Prigogine for his encouragement. We are indebted to the British Council, the Serbian Ministry of Science, and the Instituts Internationaux Solvay de Physique et de Chimie (Brussels) for financial support for this project.

References

Balescu R 1963 *Statistical Mechanics of Charged particles* (New York: Wiley-Interscience)
George C 1970 *Acad. R. Belgique, Bull. Cl. Sci.* **56** 505-19
Škarka V 1987a *Physica* **142A** 405-23
—— 1987b *Physica* **142A** 424-40
—— 1989a *Physica* **156A** 651-78
—— 1989b submitted to *Physica* A
Škarka V and Coveney P V 1988 *J. Phys. A: Math. Gen.* **21** 2595-616
—— 1990 *J. Phys. A: Math. Gen.* **23** 2439-61